



## **A thick crustal block revealed by reconstructions of early Mars highlands**

Sylvain Bouley, James Tuttle Keane, David Baratoux, Benoit Langlais, Isamu Matsuyama, F. Costard, Roger Hewins, Valérie Payré, Violaine Sautter, Antoine Séjourné, et al.

### **► To cite this version:**

Sylvain Bouley, James Tuttle Keane, David Baratoux, Benoit Langlais, Isamu Matsuyama, et al.. A thick crustal block revealed by reconstructions of early Mars highlands. *Nature Geoscience*, 2020, 13 (2), pp.105-109. <10.1038/s41561-019-0512-6>. <hal-02900960>

**HAL Id: hal-02900960**

**<https://hal.science/hal-02900960v1>**

Submitted on 16 Nov 2020

**HAL** is a multi-disciplinary open access archive for the deposit and dissemination of scientific research documents, whether they are published or not. The documents may come from teaching and research institutions in France or abroad, or from public or private research centers.

L'archive ouverte pluridisciplinaire **HAL**, est destinée au dépôt et à la diffusion de documents scientifiques de niveau recherche, publiés ou non, émanant des établissements d'enseignement et de recherche français ou étrangers, des laboratoires publics ou privés.



HAL Authorization

# A thick crustal block revealed by reconstructions of early Mars highlands

Sylvain Bouley<sup>1,2\*</sup>, James Tuttle Keane<sup>3</sup>, David Baratoux<sup>4</sup>, Benoit Langlais<sup>5</sup>, Isamu Matsuyama<sup>6</sup>, Francois Costard<sup>1</sup>, Roger Hewins<sup>7</sup>, Valerie Payré<sup>8</sup>, Violaine Sautter<sup>7</sup>, Antoine Séjourné<sup>1</sup>, Olivier Vanderhaeghe<sup>4</sup> and Brigitte Zanda<sup>2,7</sup>

**The global-scale crustal structure of Mars is shaped by impact basins, volcanic provinces, and a hemispheric dichotomy with a thin crust beneath the northern lowlands and a thick crust beneath the southern highlands. The southern highlands are commonly treated as a coherent terrain of ancient crust with a common origin and shared geologic history, plausibly originating from a giant impact(s) or a hemispheric-scale mantle upwelling. Previous studies have quantified the contribution of volcanism to this crustal structure; however, the influence of large impacts remains unclear. Here we present reconstructions of the past crustal thickness of Mars (about 4.2 Gyr ago) where the four largest impact basins (Hellas, Argyre, Isidis and Utopia) are removed, assuming mass conservation, as well as the main volcanic provinces of Tharsis and Elysium. Our reconstruction shows more subdued crustal thickness variations than at present, although the crustal dichotomy persists. However, our reconstruction reveals a region of discontinuous patches of thick crust in the southern highlands associated with magnetic and geochemical anomalies. This region, corresponding to Terra Cimmeria-Sirenum, is interpreted as a discrete crustal block. Our findings suggest that the southern highlands are composed of several crustal blocks with different geological histories. Such a complex architecture of the southern highlands is not explained by existing scenarios for crustal formation and evolution.**

The crust of Mars has been shaped by 4.5 Gyr of meteorite impacts, volcanism, tectonism and surface processes (Fig. 1a,b). Its most prominent crustal features are the hemispheric dichotomy, the Tharsis volcanic province and several large impact basins. The hemispheric dichotomy describes Mars's north–south asymmetry, where the northern lowlands have roughly half the crustal thickness of the southern highlands. The Tharsis volcanic province represents the thickest region of the crust and is associated with a prominent topographic rise responsible for deformation of the lithosphere at a planetary scale<sup>1</sup>. Whereas the crustal thickness of Tharsis is considered to be the result of magmatic intrusions and volcanic eruptions, the origin of the hemispheric dichotomy is more enigmatic. Past studies have suggested that the hemispheric crustal dichotomy is the result of either giant impact(s)<sup>2,3</sup> or hemispheric-scale mantle upwelling<sup>4,5</sup>.

While previous studies have quantified the contribution of Tharsis to Mars's gravity field<sup>1</sup>, crustal thickness<sup>6</sup> and topography<sup>7</sup>, the contribution of impact basins to the crustal structure has never been quantified. Mars has four giant (diameters >1,000 km) unequivocal impact basins with unambiguous gravity field anomalies and expressions in crustal thickness maps (Hellas, Argyre, Utopia and Isidis), but only three of them have a significant topographic expression (Hellas, Argyre and Isidis). Utopia has a muted topographic signature, due to its early formation and possible crustal relaxation<sup>8</sup>. The four impacts (Hellas, Argyre, Isidis and Utopia) predate Tharsis, and extensively modified Mars's crustal structure. For example, Hellas is surrounded by an annulus of high-standing topography and thickened crust, which has been interpreted to be

the consequence of ejecta deposits and crustal thickening during crater excavation and collapse<sup>9–11</sup> (Extended Data Fig. 1). Several outcrops in Terra Cimmeria and Terra Sirenum are interpreted as a veneer of Hellas ejecta over older crust—roughly four crater radii away from the centre of the basin<sup>12</sup>. Investigations of lunar gravity and topography, coupled with hydrocode impact simulations, have suggested that the Moon's hemispheric dichotomy (where the far-side crust is about twice as thick as the nearside crust) may be partially explained by the deposition of a thick ejecta blanket around the giant South Pole–Aitken impact basin<sup>13,14</sup>. Extrapolating these results to Mars, it appears necessary to determine the contribution of large impact basins to its present crustal structure.

## Reconstructing Mars without impact basins and volcanoes

There are many methods for isolating, characterizing and removing the contribution of impact basins and volcanoes from the gravity field and topography of planets—each with varying degrees of complexity<sup>1,6,15,16</sup>. In this work we develop a method for removing these features using crustal thickness maps<sup>17,18</sup> (Fig. 1c,d). These maps—which are derived from topography and gravity data (Methods)—can be used for reconstruction of the early crustal structure with conservation of mass arguments. The present crustal thickness model (model B, ref. <sup>18</sup>) accounts for higher crustal densities in volcanic complexes (2,900 kg m<sup>-3</sup>), lower crustal densities elsewhere (2,582 kg m<sup>-3</sup>) and a mantle density of 3,500 kg m<sup>-3</sup>. To simplify calculations, the crustal thickness was rescaled at every location to the same crustal density (that is, we increase (decrease) the crustal

<sup>1</sup>GEOPS – Géosciences Paris Sud, Univ. Paris-Sud, CNRS, Université Paris-Saclay, Orsay, France. <sup>2</sup>IMCCE – Observatoire de Paris, CNRS-UMR 8028, Paris, France. <sup>3</sup>California Institute of Technology, Pasadena, CA, USA. <sup>4</sup>Geosciences Environnement Toulouse, UMR 5563 CNRS, IRD & Université de Toulouse, Toulouse, France. <sup>5</sup>Laboratoire de Planétologie et Géodynamique, CNRS UMR 6112, Université de Nantes, Université d'Angers, Nantes, France.

<sup>6</sup>Lunar and Planetary Laboratory, University of Arizona, Tucson, AZ, USA. <sup>7</sup>Institut de Minéralogie, de Physique des Matériaux, et de Cosmochimie (IMPMC) – Sorbonne Université– Muséum National d'Histoire Naturelle, UPMC Université Paris 06, UMR CNRS 7590, IRD UMR 206, Paris, France.

<sup>8</sup>Department of Earth, Environmental and Planetary Sciences, Rice University, Houston, TX, USA. \*e-mail: [sylvain.bouley@u-psud.fr](mailto:sylvain.bouley@u-psud.fr)



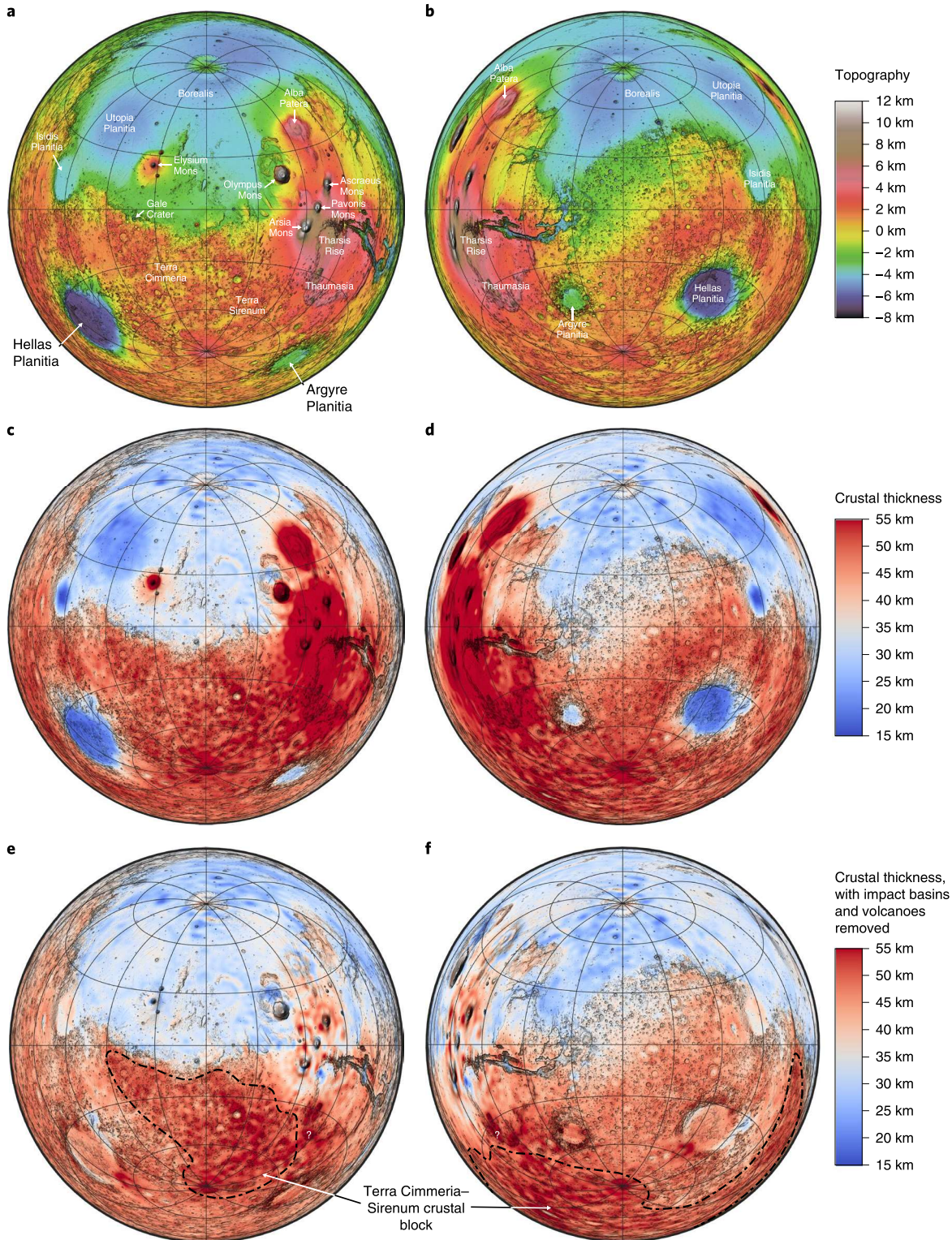


**Fig. 1 | A global view of the crustal structure of Mars. a,b,** The Mars Orbiter Laser Altimeter topography of Mars with the features of interest labelled<sup>9</sup>. **c,d,** The crustal thickness of Mars based on crustal model B (ref. <sup>18</sup>, Methods). **e,f,** The crustal thickness of Mars after removing all of the large impact basins and volcanic features. The Cimmeria-Sirenum crustal block is enclosed by a dash-dot line. The question mark to the east of the block indicates the unclear boundary between the Thaumasia region and the Cimmeria-Sirenum block due to the possible specific origin of Thaumasia<sup>9</sup>. The maps are in Lambert azimuthal equal-area projection, centred on the equator at longitudes 0° (left column) and 180° (right column). Each map covers all of Mars except for a small region antipodal to the map centre. The maps are overlaid on the present-day topography for reference. Grid lines are in increments of 30° of latitude and longitude.

thickness in regions of high (low) density until the crustal density is globally uniform). This lets us use crustal mass and crustal volume conservation interchangeably.

We assume that impacts and volcanoes modify the crustal structure symmetrically about their centres, and that impact basins reshape the crust in a manner that approximately conserves crustal

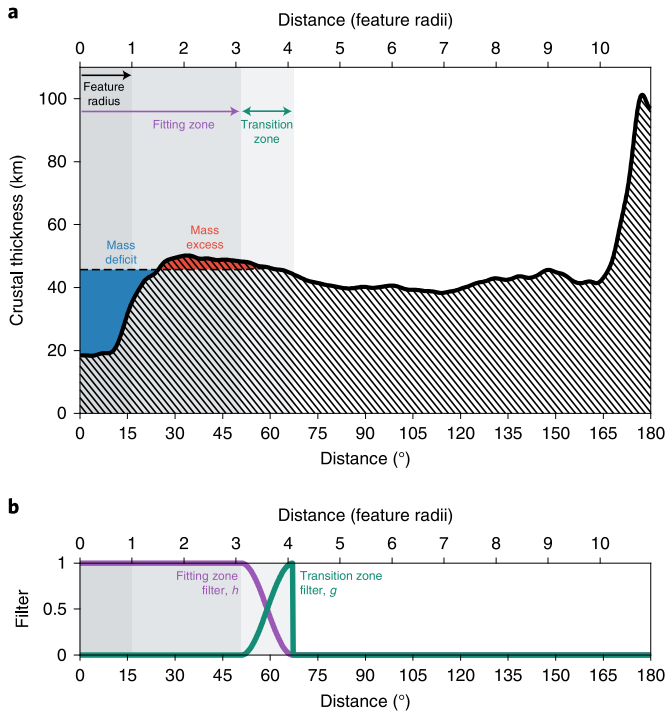


**Fig. 2 | The radial crustal structure of Hellas Planitia. a**, The azimuthally average crustal thickness about Hellas (solid black line with hatching beneath). We calculate the mean crustal thickness in the transition zone, and then calculate the mass of crustal material above and below that datum within the 'fitting zone'. The mass above the mass-conserving crustal thickness (the mass excess, red) integrated in an annulus around the feature is equal to the mass below it (the mass deficit, blue). The peak at 180° distance is Alba Patera, which is approximately antipodal to Hellas. **b**, The fitting and transition zone filters used in this reconstruction (Methods).

mass. Figure 2 shows an example of our fitting process for the Hellas basin. To remove the feature of interest, we first calculate the azimuthally averaged crustal thickness as a function of distance from the centre of the feature (Fig. 2a). Next, we define an annulus outside the feature (the 'transition zone', Fig. 2a,b), which we take to represent the background crustal thickness. We calculate the mean crustal thickness in the transition zone, and then calculate the mass of crustal material above and below that datum within the 'fitting zone'. If the mass above the datum (the mass excess) equals the mass below the datum (the mass deficit), then we deem the background crustal thickness to be a mass-conserving solution. We include a cosine taper to prevent discontinuities in the corrected crustal thickness map. For each feature of interest, we performed a parameter-space search for mass-conserving crustal structure corrections—testing a range of possible transition zone radii and widths (Extended Data Fig. 3). In cases where multiple mass-conserving solutions are found, we select the solution that makes the smallest change to the crustal structure. In cases where no mass-conserving solution is found, we select the solution that comes closest to conserving mass. While the formation of impact basins should conserve crustal mass, the same cannot be assumed for large volcanic edifices (as the erupted mass may be derived from the mantle and not the crust). Thus, for removing volcanoes, we prescribe a nominal angular radius of the feature based on the slope break at its edge that is identified on the azimuthally averaged crustal thickness profiles. We then remove the crustal mass above the background, defined from an average value in an annulus surrounding the volcanic province (Extended Data Fig. 4).

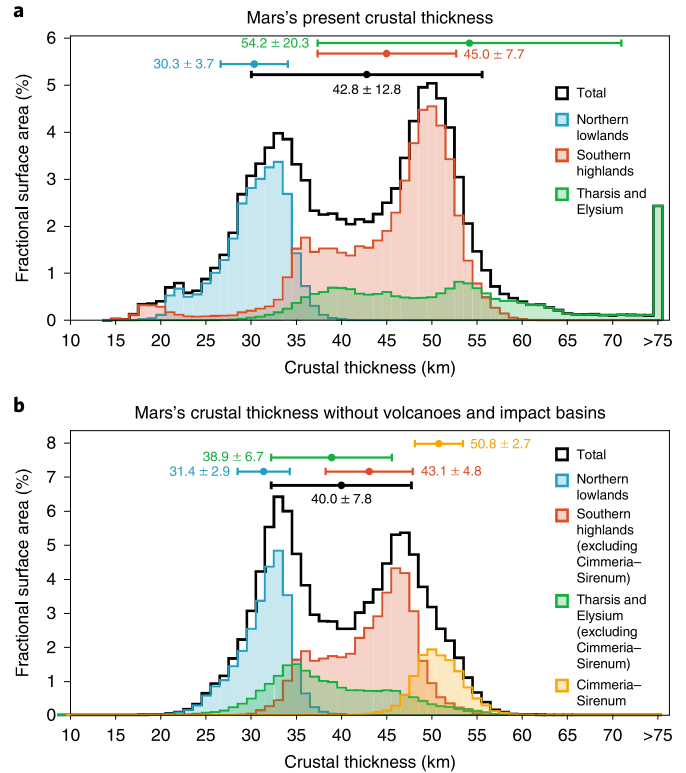


**Fig. 3 | Histograms of crustal thickness of three domains (northern lowlands, southern highlands and Cimmeria-Sirenum) of the Martian crust. a**, Mars's present crustal thickness. **b**, Mars's crustal thickness without volcanoes and impact basins. Note that the contribution of Tharsis and Elysium is isolated to the northern lowlands to visualize the residual contribution after removal. The black histograms show the global distribution of crustal thickness; when summed together, those coloured histograms equal the global histogram. The horizontal error bars indicate the mean and standard deviation for each respective distribution.

Using this technique, we sequentially isolated and removed the axisymmetric crustal thickness structures associated with the four largest impact basins (Hellas (Fig. 2), Argyre, Isidis and Utopia), Elysium Mons and the Tharsis Rise, plus the five largest individual volcanoes: Olympus Mons, Arsia Mons, Pavonis Mons, Ascraeus Mons and Alba Patera. This method is iterative and nonlinear. That is, starting with the present crustal thickness of Mars, we remove one feature, and then use that iterated crustal thickness as the starting point for removing the next feature, and so on (Extended Data Fig. 5). This means that the resulting corrected crustal structure depends a priori on the order in which we remove features, although the effect of the order is minimal if the features are distant enough from each other, which is the case here. To evaluate this dependence, we repeated this analysis using randomized removal sequences. We find that the solution is only weakly dependent on the order of removal (Methods). With this precaution taken, our nominal solution uses a removal sequence based on our current knowledge of the relative chronology of basins and volcanoes<sup>8</sup>, from youngest to oldest: Elysium, Olympus and Tharsis montes, Tharsis Rise, Argyre, Isidis, Hellas and Utopia.

### Subdued thickness variations of the early Martian crust

Removing impact basins and volcanic constructs reveals more subdued crustal thickness variations (Figs. 1e,f and 3). The hemispheric dichotomy persists in the reconstruction. Hellas contributes to the southern highlands, but excavation of the basin and emplacement



of ejecta are unable to explain the entire dichotomy; the mass excess in the southern highlands is about four times larger than the mass deficit within the Hellas basin.

However, after removing all of the large impact basins and volcanic features, the crustal thickness map highlights a crustal block characterized by discontinuous, thick (>50 km) regions corresponding to Terra Cimmeria–Sirenum (Fig. 1e,f). We delineated the boundary of this block such that it includes all of the neighbouring >50-km-thick crustal segments (Extended Fig. 6). We excluded the Thaumasia region, even though it has comparable thickness, because it may have a different tectonic (orogenic) history<sup>19</sup>. The relation between the most eastern part of the Terra Cimmeria–Sirenum crustal block and Thaumasia is unclear (Fig. 1e,f).

The distribution of crustal thicknesses suggests that the early Martian crust can be divided into three main crustal domains having characteristic thickness ranges that partially overlap (Fig. 3b): the northern lowlands with a thickness of between 20 and 38 km (centred at 33 km); the southern highlands—including Arabia Terra, Hellas and Argyre—with an intermediate thickness of between 30 and 55 km (centred at 46 km); and the Terra Cimmeria–Sirenum block with a thickness of between 42 and 60 km (centred at 50 km).

### A thick crustal block in the southern highlands

The Cimmeria–Sirenum crustal block is also noticeable because it shares many of the characteristics of terrestrial continental crust. On Earth, continental crust is derived via differentiation and remelting of pre-existing basaltic crust. It possesses an intermediate composition between felsic and mafic, is enriched in incompatible elements, and is associated with thicker crust and elevated topography. The Terra Cimmeria–Sirenum region is associated with anomalously elevated pre-Tharsis topography<sup>20</sup> (Extended Data Fig. 7) and includes the strongest crustal magnetic anomalies<sup>21–24</sup> (Fig. 4a), which, by comparison with the Earth, could correspond to the accretion of terranes<sup>25</sup>. Terra Cimmeria–Sirenum is also associated with some of the highest surface (down to the first metre) abundances of potassium (K) and thorium (Th) (Fig. 4b,c)<sup>26</sup>. This region is the only place in the southern terrains where K and Th are correlated. Within this region, lower concentrations of K and Th are noted in the region near the south pole, where ground ice may mask the true (ice-free) K and Th (ref. <sup>26</sup>). Only the most eastern part of the crustal block (~10% of its surface area) is not associated with these geochemical and magnetic anomalies. Possible fragments of continental crust have been found with *in situ* observations by the Curiosity rover at Gale crater<sup>27</sup> on the northern edge of the Cimmeria–Sirenum block (Fig. 1a). While this interpretation appears inconsistent with the vast amount of spectroscopic observations suggesting that the surface of this region is dominated by basaltic rock<sup>28</sup>, it is plausible that these basalts are surficial deposits overlying a geochemically distinct crust. This would explain why exposed continental components are rare in the southern hemisphere<sup>29</sup>.

The existence of (at least) one crustal block on Mars makes the pre-Noachian geologic history of Mars—and the origin of the hemispheric dichotomy—much more complex than previously recognized. We identify a regional-scale crustal block covering 10% of Mars. Geophysical and geochemical signatures in this region

are suggestive of a geochemically evolved crustal component. Combined with the identification of continental crust-like material on Mars in specific outcrops<sup>30</sup>, and inferred from meteoritic samples containing zircons<sup>27,31,32</sup>, our findings suggest that the Cimmeria–Sirenum crustal block had a complex geologic history, whether or

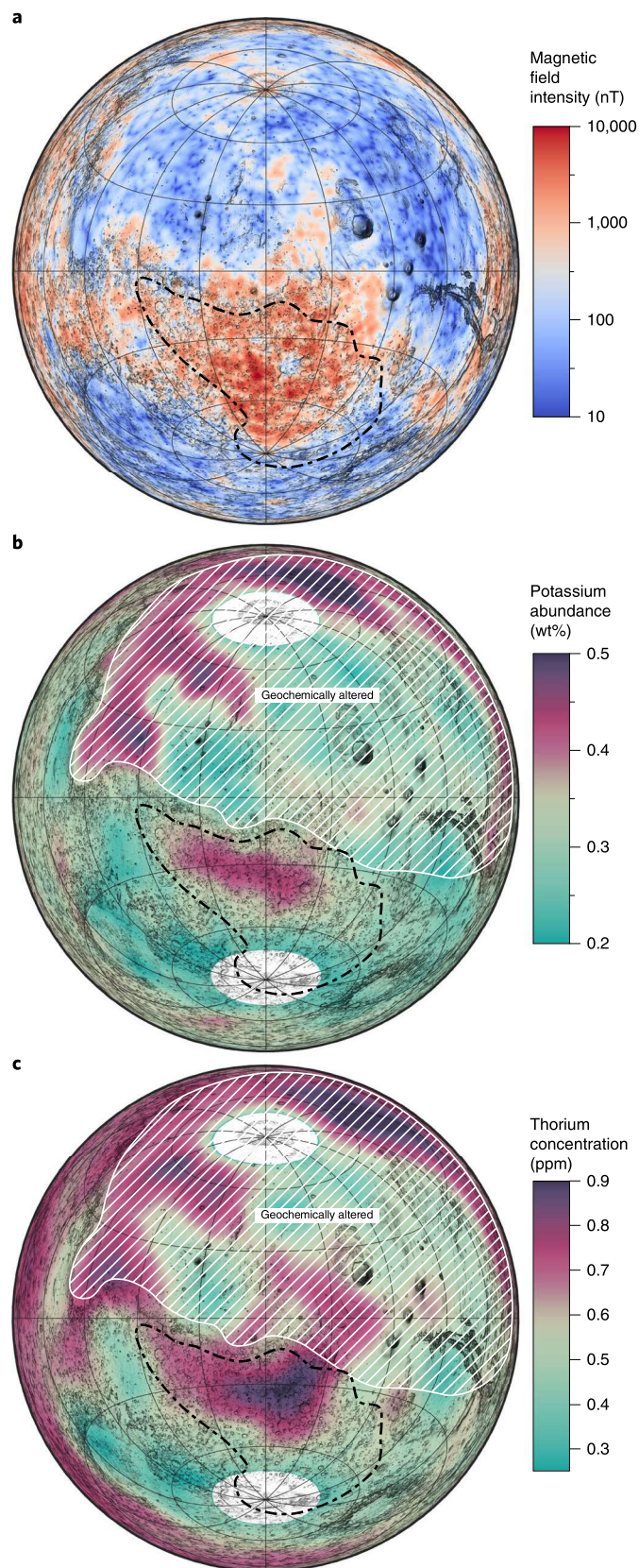


**Fig. 4 | The geophysical and geochemical signature of the Cimmeria–Sirenum block. a,** The magnetic field intensity, evaluated at the surface of Mars<sup>24</sup>. **b,** The potassium concentration (wt%)<sup>26</sup>. **c,** The thorium concentration (ppm)<sup>26</sup>. In **b** and **c**, the northern hemisphere is hatched out to focus attention on the signatures south of the dichotomy. The maps are in Lambert azimuthal equal-area projection, centred on 0°, and cover all of Mars except for a small region on the opposite hemisphere. The maps are overlaid on the present-day topography for reference. The Cimmeria–Sirenum crustal block is enclosed by a dash-dot line.

not it is analogous to terrestrial continental crust. Since this terrain is overprinted by the Hellas and Argyre basins, it is probably the oldest part of the crust. Subsequent large impacts significantly altered Mars's crustal structure and contributed to the observed hemispheric dichotomy. Therefore, the southern highlands should not be considered as a single, homogeneous unit (requiring a single formation mechanism), but rather a collection of crustal blocks with plausibly different origins, variably affected by magmatic, tectonic and impact processes. The formation mechanism of several crustal blocks during the pre-Noachian (before 4.1 Gyr ago) remains to be deciphered and has important implications for the planet's evolution, including its climate, the surface environment and the mantle dynamics.

## Online content

Any methods, additional references, Nature Research reporting summaries, source data, extended data, supplementary information, acknowledgements, peer review information; details of author contributions and competing interests; and statements of data and code availability are available at <https://doi.org/10.1038/s41561-019-0512-6>.

Received: 26 January 2019; Accepted: 19 November 2019;

Published online: 6 January 2020

## References

1. Zuber, M. T. & Smith, D. E. Mars without Tharsis. *J. Geophys. Res.* **102**, 28673–28686 (1997).
2. Wilhelms, D. E. & Squyres, S. W. The martian hemispheric dichotomy may be due to a giant impact. *Nature* **309**, 138–140 (1984).
3. Frey, H. & Shultz, R. A. Large impact basins and the mega-impact origin for the crustal dichotomy on Mars. *Geophys. Res. Lett.* **15**, 229–232 (1988).
4. Zhong, S. & Zuber, M. T. Degree-1 mantle convection and the crustal dichotomy on Mars. *Earth Planet. Sci. Lett.* **189**, 75–84 (2001).
5. Roberts, J. H. & Zhong, S. Degree-1 convection in the Martian mantle and the origin of the hemispheric dichotomy. *J. Geophys. Res.* **111**, E06013 (2006).
6. Andrews-Hanna, J. C., Zuber, M. T. & Banerdt, W. B. The Borealis basin and the origin of the martian crustal dichotomy. *Nature* **453**, 1212–1215 (2008).
7. Matsuyama, I. & Manga, M. Mars without the equilibrium rotational figure, Tharsis, and the remnant rotational figure. *J. Geophys. Res. Planets* **115**, 12020 (2010).
8. Fassett, C. I. & Head, J. W. Sequence and timing of conditions on early Mars. *Icarus* **211**, 1204–1214 (2011).
9. Smith, D. E. et al. The global topography of Mars and implications for surface evolution. *Science* **284**, 1495–1503 (1999).
10. Zuber, M. T. et al. Internal structure and early thermal evolution of Mars from Mars Global Surveyor topography and gravity. *Science* **287**, 1788–1793 (2000).
11. Zuber, M. The crust and mantle of Mars. *Nature* **412**, 220–227 (2001).
12. Irwin, R. P., Tanaka, K. L. & Robbins, S. J. Distribution of Early, Middle, and Late Noachian cratered surfaces in the Martian highlands: implications for resurfacing events and processes. *J. Geophys. Res. Planets* **118**, 278–291 (2013).
13. Melosh, H. J. et al. South Pole–Aitken basin ejecta reveal the Moon's upper mantle. *Geology* **45**, 1063–1066 (2017).
14. Zuber, M. T., Smith, D. E., Lemoine, F. G. & Neumann, G. A. The shape and internal structure of the Moon from the Clementine mission. *Science* **266**, 1839–1843 (1994).
15. Keane, J. T. & Matsuyama, I. Evidence for lunar true polar wander and a past low-eccentricity, synchronous lunar orbit. *Geophys. Res. Lett.* **41**, 6610–6619 (2014).
16. Garrick-Bethell, I., Perera, V., Nimmo, F. & Zuber, M. T. The tidal-rotational shape of the Moon and evidence for polar wander. *Nature* **512**, 181–184 (2014).
17. Genova, A. et al. Seasonal and static gravity field of Mars from MGS, Mars Odyssey and MRO radio science. *Icarus* **272**, 228–245 (2016).
18. Goossens, S. et al. Evidence for a low bulk crustal density for Mars from gravity and topography. *Geophys. Res. Lett.* **44**, 7686–7694 (2017).
19. Nahm, A. L. & Schultz, R. A. Evaluation of the orogenic belt hypothesis for the formation of the Thaumasia highlands, Mars. *J. Geophys. Res.* **115**, E04008 (2010).
20. Bouley, S. et al. Late Tharsis formation and implications for early Mars. *Nature* **531**, 344–347 (2016).
21. Connerney, J. E. P. et al. The global magnetic field of Mars and implications for crustal evolution. *Geophys. Res. Lett.* **28**, 4015–4018 (2001).
22. Arkani-Hamed, J. A coherent model of the crustal magnetic field of Mars. *J. Geophys. Res.* **109**, E09005 (2004).
23. Langlais, B., Purcher, M. E. & Manda, M. Crustal magnetic field of Mars. *J. Geophys. Res.* **109**, E02008 (2004).
24. Langlais, B. et al. A new model of the crustal magnetic field of Mars using MGS and MAVEN. *J. Geophys. Res. Planets* **124**, 1542–1569 (2019).
25. Fairén, A. G., Ruiz, J. & Anguita, F. An origin for the linear magnetic anomalies on Mars through accretion of terranes: implications for dynamo timing. *Icarus* **160**, 220–223 (2002).
26. Boynton, W. V. et al. Concentration of H, Si, Cl, K, Fe, and Th in the low- and mid-latitude regions of Mars. *J. Geophys. Res.* **112**, E12S99 (2007).
27. Sautter, V. et al. In situ evidence for continental crust on early Mars. *Nat. Geosci.* **8**, 605–609 (2015).
28. Rogers, A. D. et al. Global spectral classification of Martian low-albedo regions with Mars Global Surveyor Thermal Emission Spectrometer (MGS-TES) data. *J. Geophys. Res.* **112**, E02004 (2007).
29. Baratoux, D. et al. Petrological constraints on the density of the Martian crust. *J. Geophys. Res. Planets* **119**, 1707–1727 (2014).
30. Christensen, P. R. et al. Evidence for magmatic evolution and diversity on Mars from infrared observations. *Nature* **436**, 504–509 (2005).
31. Humayun, M. et al. Origin and age of the earliest Martian crust from meteorite NWA 7533. *Nature* **503**, 513–516 (2013).
32. Bouvier, L. C. et al. Evidence for extremely rapid magma ocean crystallization. *Nature* **586**, 586–589 (2018).